Polarizabilities of Nonreciprocal Bianisotropic Particles

M. S. Mirmoosa, Y. Ra'di, V. S. Asadchy, C. R. Simovski, and S. A. Tretyakov

Department of Radio Science and Engineering, School of Electrical Engineering, Aalto University, P.O. Box 13000, FI-00076 Aalto, Finland

(Received 24 February 2014; published 28 April 2014)

The most general response of a small dipolar particle to electromagnetic fields is determined not by its electric and magnetic polarizabilities only but also by magnetoelectric coupling coefficients. We are interested in creating particles with engineered magnetoelectric coupling of nonreciprocal nature, including artificial "moving particles." Recently, it has been shown theoretically that using small nonreciprocal bianisotropic particles, one can realize perfect electromagnetic isolators, nonreciprocal twist polarizers, one-way transparent sheets, and other devices. This paper is a necessary step towards these applications. For two electrically small nonreciprocal scatterers, an analytical electromagnetic model of polarizabilities is developed. Both particles are bianisotropic: the so-called Tellegen omega particle and moving chiral particle. Analytical results are compared to the full-wave numerical simulations. Both models satisfy to main physical restrictions and leave no doubts in the possibility to realize these particles experimentally.

DOI: 10.1103/PhysRevApplied.1.034005

I. INTRODUCTION

In terms of electromagnetic properties of materials, the most general linear material is the bianisotropic medium in which the relations between the four field vectors **E**, **H**, **D**, and **B** are defined by four general dyadic coefficients, as in

$$\begin{bmatrix} \mathbf{D} \\ \mathbf{B} \end{bmatrix} = \begin{bmatrix} \bar{\bar{\epsilon}} & \bar{\bar{\alpha}} \\ \bar{\bar{\beta}} & \bar{\bar{\mu}} \end{bmatrix} \cdot \begin{bmatrix} \mathbf{E} \\ \mathbf{H} \end{bmatrix} \tag{1}$$

(see, e.g., Ref. [1]). Obviously, only a limited range of material parameters is accessible in natural materials, and researchers have made significant efforts in synthesizing artificial composite materials with novel electromagnetic properties not found in any natural substance. This is achieved by engineering electrically small particles which respond to electromagnetic excitations as electric and magnetic dipoles in the desired way. The most general bianisotropic material can be conceptually realized as a mixture of many small inclusions modeled by the most general bianisotropic relations between the induced moments and exciting fields:

$$\begin{bmatrix} \mathbf{p} \\ \mathbf{m} \end{bmatrix} = \begin{bmatrix} \bar{\bar{\alpha}}_{\mathrm{ee}} & \bar{\bar{\alpha}}_{\mathrm{em}} \\ \bar{\bar{\alpha}}_{\mathrm{me}} & \bar{\bar{\alpha}}_{\mathrm{mm}} \end{bmatrix} \cdot \begin{bmatrix} \mathbf{E} \\ \mathbf{H} \end{bmatrix}. \tag{2}$$

Here, **p** and **m** are the induced electric and magnetic dipole moments, respectively, and $\bar{\bar{\alpha}}_{\mathrm{ij}}$ are the polarizability dyadics. In the modern literature, this concept is called the metamaterial concept, and small engineered inclusions in these composites are called meta-atoms. In the past, significant results have been achieved in realizing artificial media with strong chirality (reciprocal magnetoelectric coupling measured by the trace of $\bar{\bar{\alpha}}_{\mathrm{em}} = -\bar{\bar{\alpha}}_{\mathrm{me}}^{T}$) and in engineering permittivity and permeability (values of $\bar{\bar{\alpha}}_{\mathrm{ee}}$ and $\bar{\bar{\alpha}}_{\mathrm{mm}}$) creating artificial magnetics and double-negative media. Reviews of recent developments in artificial chiral materials can be found in Refs. [2,3].

In this paper, we focus on the problem of the realization and optimization of the magnetoelectric coefficients which determine nonreciprocal mechanisms of magnetoelectric coupling. The main motivations of this research are recent discoveries of extreme properties of nonreciprocal bianisotropic particles [4,5], such as extreme asymmetry in scattering response (invisible from one of the directions, optimal absorption from the opposite direction, etc). It is understood that planar arrays of small nonreciprocal bianisotropic particles with special values of the coupling coefficients can be used as transparent absorbing boundaries [6] (which were introduced earlier for the termination of computational domains in finite-element methods [7]). Furthermore, such arrays can be applied for novel implementations of perfect electromagnetic isolators [8], twist polarizers [9], thin-sheet phase shifters, and other devices [10,11]. An artificial moving medium with properly chosen values of the material parameters can transform electromagnetic fields in a very general manner [12]. However, at this time, all these applications are only theoretical predictions. Scatterers with the desired parameter values do not exist in nature, and there are no known realizations of nonreciprocal bianisotropic meta-atoms. In this paper, we develop an analytical model of two nonreciprocal meta-atoms, which realize nonreciprocal field coupling of both fundamental classes: Tellegen and "moving-particle" coupling [1]. The results show that desired novel effects can be achieved in particles made of conventional materials and have reasonable dimensions.

The nonreciprocity of media in applied dc magnetic fields or media with spontaneous magnetization is

commonplace in classical electrodynamics. This nonreciprocity obviously implies anisotropy of the medium and is related to the off-diagonal components of the permittivity (magneto-optical media, magnetized plasmas) or permeability (gyrotropic media, e.g., ferrites) dyadics. On the other hand, nonreciprocal effects in bianisotropic media due to the nonreciprocal nature of magnetoelectric interactions in the medium (see, e.g., Ref. [1]) are very rare and very weak. For example, the Tellegen coupling has been observed in some antiferromagnetic crystals at low frequencies [13]. It is clear that the metamaterial concept is the only possible route towards realization of nonreciprocal particles offering the theoretically expected extreme performance.

In 1948, Tellegen suggested an idea of an electromagnetic gyrator, a general nonreciprocal four pole [14]. In electromagnetics, the gyrator element corresponds to a nonreciprocal particle with nonzero trace of $\bar{\bar{\alpha}}_{\mathrm{em}} = \bar{\bar{\alpha}}_{\mathrm{me}}^{T}$, and to composite media (Tellegen's medium) performed as a random mixture of such particles. Sihvola conceptualized a microscopic particle with permanent electric and magnetic dipole moments parallel to one another and linked by a nonelectromagnetic force [15]. The coupling of electric and magnetic polarizations in such composite is of nonreciprocal nature. However, practical possibilities to create the Tellegen particle and medium remain problematic. In 1996, Kamenetskii [16] suggested magnetostatic ferrite resonators shaped as tablets with partial metallization (shaped as a strip) on one side of the tablet as a conceptual nonreciprocal bianisotropic particle. Ferrite disks of small sizes compared to the wavelength operate as very compact resonators of magnetostatic waves because of dramatic shortening of these waves compared to the electromagnetic wave in free space at the same frequency. In that work, Kamenetskii predicted that a chain of such tablets should operate as a nonreciprocal bianisotropic waveguide [16]. He has shown that it should be possible to obtain a controllable coupling coefficient of nonreciprocal tablets simply by tuning the bias magnetic field. In 1998, Dmitriev [17] generalized the results by Kamenetskii to a hypothetic medium which represented an anisotropic variant of the Tellegen medium and showed topologies which corresponded to the other fundamental class of nonreciprocal bianisotropic coupling: the "moving" particle. In 1998, Tretyakov [18] introduced two designs of anisotropic nonreciprocal scatterers which presumably possessed more significant resonant nonreciprocity of their polarizabilities than the tablets of Kamenetskii.

In 2003, the group of Tretyakov experimentally confirmed the existence of nonreciprocal magnetoelectric coupling [19] in one of the configurations introduced in Ref. [18], but in that work, the particle polarizability value was not determined, and there was no model to predict and optimize the particle response. In the present paper, we make an important step towards realization of nonreciprocal bianisotropic meta-atoms with desired values of the polarizabilities, developing an analytical model which allows us to predict the polarizability values of particles with given topology and dimensions.

II. THEORY

The geometry of the considered artificial nonreciprocal bianisotropic particles [18,20] is shown in Figs. 1(a) (Tellegen omega) and 1(b) (moving chiral). The operation principle of both of them is that a local (external with respect to the particle) high-frequency electric field excites currents in the metal wires, and the magnetic field created by the electric current of these wires induces a magnetic moment in the ferrite sphere. This way, a nonreciprocal magnetoelectric coupling is realized. Likewise, a local high-frequency magnetic field applied to the ferrite sample causes its high-frequency magnetization, which, in turn, induces an electric current and electric dipole moment in the metal wires.

The general relation between the local fields and induced dipole moments is given by Eq. (2). The Tellegen omega and moving chiral particles, as the suggested nonreciprocal bianisotropic particles, are uniaxial. Therefore, we can write the polarizability dyadics of these two particles in the form

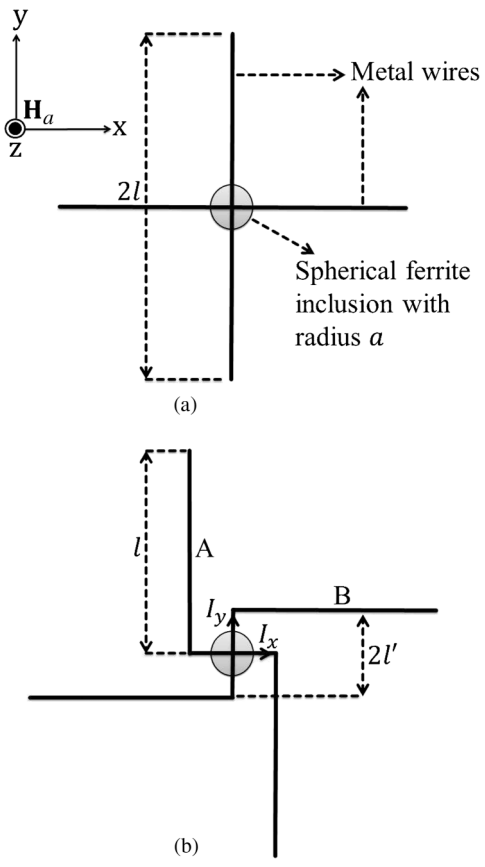

FIG. 1. Geometry of the (a) Tellegen omega particle and (b) moving chiral particle. The applied bias magnetic field ($\mathbf{H}_a$) is directed along the $\mathbf{z}_0$ axis.

$$\bar{\bar{\alpha}}_{ee} = \alpha_{ee}^{co}\bar{\bar{I}}_t + \alpha_{ee}^{cr}\bar{\bar{J}}_t, \qquad \bar{\bar{\alpha}}_{mm} = \alpha_{mm}^{co}\bar{\bar{I}}_t + \alpha_{mm}^{cr}\bar{\bar{J}}_t,$$
$$\bar{\bar{\alpha}}_{em} = \alpha_{em}^{co}\bar{\bar{I}}_t + \alpha_{em}^{cr}\bar{\bar{J}}_t, \qquad \bar{\bar{\alpha}}_{me} = \alpha_{me}^{co}\bar{\bar{I}}_t + \alpha_{me}^{cr}\bar{\bar{J}}_t. \tag{3}$$

Here, $\bar{\bar{I}}_t = \bar{\bar{I}} - \mathbf{z}_0\mathbf{z}_0$ is the transverse unit dyadic, $\bar{\bar{I}}$ is the 3D unit dyadic, and $\bar{\bar{J}}_t = \mathbf{z}_0 \times \bar{\bar{I}}_t$ is the vector-product operator.

A. Tellegen omega particle

The geometry of the particle is shown in Fig. 1(a). Two metal wires (or strips) and a ferrite inclusion constitute the particle.

The Tellegen omega particle is one of those two particles which have been introduced as artificial nonreciprocal bianisotropic particles. It is clear from the particle name that it simultaneously exhibits two electromagnetic coupling effects: nonreciprocal Tellegen and reciprocal omega coupling.

1. Electric and magnetoelectric polarizabilities

We assume that the Tellegen omega particle is excited by a uniform $\mathbf{x}_0$-directed electric field. This external field induces an electric current in the metal wire which is in the direction of the electric field. Assuming that the wire length is much smaller than the wavelength ($l \ll \lambda$), the current distribution in the wire is approximated as [21]

$$I_x = I_{0x}\frac{\cos(kx) - \cos(kl)}{1 - \cos(kl)} \approx I_{0x}\left(1 - \frac{x^2}{l^2}\right), \tag{4}$$

where

$$I_{0x} = \frac{2\tan\left(\frac{kl}{2}\right)}{kZ_{in}}E \approx \frac{l}{Z_{in}}E. \tag{5}$$

E is the peak value of the incident electric field, k is the free-space wave number, and Z_{in} represents the input impedance of a linear electric dipole antenna. For such an antenna, the input admittance can be expressed as [22]

$$Y_{in} = 2\pi j\frac{kl}{\eta\Psi}\left[1 + k^2l^2\frac{F}{3} - jk^3l^3\frac{1}{3(\Omega - 3)}\right],$$
$$F = 1 + \frac{1.08}{\Omega - 3}, \qquad \Omega = 2\log\frac{2l}{r_0},$$
$$\Psi = 2\log\frac{l}{r_0} - 2, \tag{6}$$

in which η is the free-space wave impedance, l is half of the length of the metal wire, and r_0 represents the wire radius. The induced electric current generates a magnetic field. By applying the Biot-Savart law in the magnetostatic approximation [23–25], the magnetic field close to the wire can be written as

$$\mathbf{H} = \int_{-l}^{+l}\frac{\mathbf{I_x dl}\times\mathbf{r}'}{r'^3} = \frac{I_{0x}(l^2 - x^2)}{4\pi Rl^2}\left(\frac{l + x}{\sqrt{R^2 + (l + x)^2}} + \frac{l - x}{\sqrt{R^2 + (l - x)^2}}\right)(-\sin\phi\,\mathbf{y}_0 + \cos\phi\,\mathbf{z}_0). \tag{7}$$

As shown in Fig. 2, $\mathbf{r}'$ is the distance vector from a differential element to the observation point A. R and ϕ are the cylindrical coordinates in the $\mathbf{y}_0\mathbf{z}_0$ plane. The $\mathbf{y}_0$ component of the magnetic field generated by the induced current in the wire excites the ferrite sphere. As it is seen from Eq. (7), this component is not uniform over the ferrite sphere volume. Hence, it is necessary to take its volume average to find the equivalent uniform external magnetic field exciting the ferrite sphere because the fundamental mode of magnetization oscillations is characterized by the uniform magnetization over the sphere volume. By assuming that the ferrite sphere is small, the averaged $\mathbf{y}_0$ component of the magnetic field can be achieved as

$$H_{y\ \text{average}} = \frac{1}{V}\int_V H_y dv = \frac{2a^2}{3V}I_{0x}. \tag{8}$$

For a ferrite sphere with the saturation magnetization along the $\mathbf{z}_0$ axis, the components of the magnetic moment are related to the external rf magnetic field as [26]

$$m_x = V\left(\frac{\alpha}{\alpha^2 + \beta^2}\chi_{xx} + \frac{\beta}{\alpha^2 + \beta^2}\chi_{xy}\right)H_{xe} + V\left(\frac{\alpha}{\alpha^2 + \beta^2}\chi_{xy} - \frac{\beta}{\alpha^2 + \beta^2}\chi_{xx}\right)H_{ye},$$
$$m_y = V\left(\frac{-\alpha}{\alpha^2 + \beta^2}\chi_{xy} + \frac{\beta}{\alpha^2 + \beta^2}\chi_{xx}\right)H_{xe} + V\left(\frac{\alpha}{\alpha^2 + \beta^2}\chi_{xx} + \frac{\beta}{\alpha^2 + \beta^2}\chi_{xy}\right)H_{ye}. \tag{9}$$

Here,

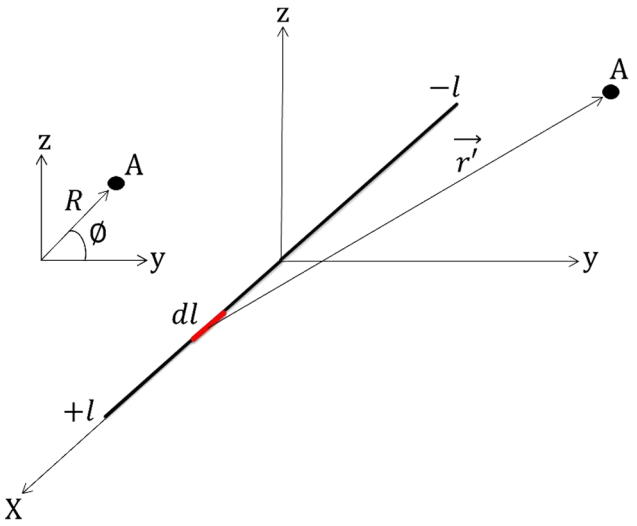

FIG. 2. The wire along the $\mathbf{x}_0$ axis is excited by the incident electric field.

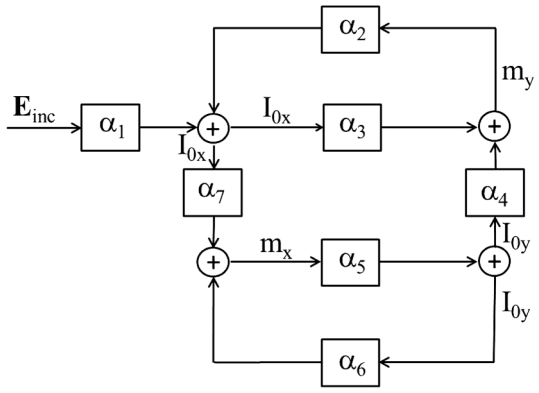

FIG. 3. Block diagram of the coupling between the ferrite inclusion and the metal wires in the Tellegen omega particle in the presence of an incident electric field in the $\mathbf{x}_0$ direction.

$$\alpha = 1 + \frac{1}{3}\chi_{xx}, \qquad \beta = \frac{1}{3}\chi_{xy}, \tag{10}$$

and H_{xe}, H_{ye} are the $\mathbf{x}_0$ and $\mathbf{y}_0$ components of the external magnetic field. Susceptibility elements are given by Refs. [26,27] for a lossy ferrite material. The averaged $\mathbf{y}_0$ component of the magnetic field produced by the wire along the $\mathbf{x}_0$ axis excites two nonzero components of the magnetic moment. These components are orthogonal to the bias field. The excited magnetic moment induces electric current in the wires. The $\mathbf{y}_0$ and $\mathbf{x}_0$ components of the magnetic moment cause the electric current induction on the $\mathbf{x}_0$- and $\mathbf{y}_0$-directed wires, respectively. The electric currents at the center of the wires, due to the magnetic moment, can be written as

$$\begin{aligned} I_{0x} &= \frac{1}{Z_{\text{in}}}\int_{-l}^{+l} E_x\left(1 - \frac{|x|}{l}\right)dx = +\frac{\xi}{Z_{\text{in}}}m_y, \\ I_{0y} &= \frac{1}{Z_{\text{in}}}\int_{-l}^{+l} E_y\left(1 - \frac{|y|}{l}\right)dy = -\frac{\xi}{Z_{\text{in}}}m_x, \end{aligned} \tag{11}$$

where ξ is an unknown coefficient. After determining all the polarizabilities, the Onsager-Casimir principle [28–30] allows us to determine this unknown coefficient. E_x and E_y represent the tangential to the wires electric field components generated by the magnetic moment. The excited wire along the $\mathbf{y}_0$ axis produces an $\mathbf{x}_0$-directed magnetic field. Similar to the adjacent wire, the volume average of this component of the magnetic field over the ferrite sphere volume can be expressed as

$$H_{x\ \text{average}} = -\frac{2a^2}{3V}I_{0y}. \tag{12}$$

Defining

$$\begin{aligned} C_{xx} = C_{yy} &\triangleq \frac{2a^2}{3}\left(\frac{\alpha}{\alpha^2+\beta^2}\chi_{xx} + \frac{\beta}{\alpha^2+\beta^2}\chi_{xy}\right), \\ C_{xy} = -C_{yx} &\triangleq \frac{2a^2}{3}\left(\frac{\alpha}{\alpha^2+\beta^2}\chi_{xy} - \frac{\beta}{\alpha^2+\beta^2}\chi_{xx}\right), \end{aligned} \tag{13}$$

and considering Eqs. (8), (9), and (12), the magnetic moment components in terms of the electric currents at the center of the wires can be written as

$$m_x = C_{xy}I_{0x} - C_{xx}I_{0y}, \qquad m_y = C_{yy}I_{0x} - C_{yx}I_{0y}. \tag{14}$$

As a result, it can be stated that there is a cyclic action, meaning that the electric currents excite the ferrite inclusion, and at the same time, the magnetic moment excites the wires. This process can be modeled by a block diagram, which can illustrate the relations between the currents and the magnetic moment components. Figure 3 shows the corresponding coupling block diagram. Also, the cycle can be modeled by the following equations:

$$\begin{aligned} I_{0x} &= \alpha_1 E + \alpha_2 m_y, & m_y &= \alpha_3 I_{0x} + \alpha_4 I_{0y}, \\ I_{0y} &= \alpha_5 m_x, & m_x &= \alpha_6 I_{0y} + \alpha_7 I_{0x}, \end{aligned} \tag{15}$$

where

$$\begin{aligned} &\alpha_1 \approx \frac{l}{Z_{\text{in}}}, \qquad \alpha_2 = -\alpha_5 = \frac{\xi}{Z_{\text{in}}}, \qquad \alpha_3 = C_{yy}, \\ &\alpha_4 = -C_{yx}, \qquad \alpha_6 = -C_{xx}, \qquad \alpha_7 = C_{xy}. \end{aligned} \tag{16}$$

Knowing that the electric dipole moments and the electric currents at the center of the electrically small short-circuit wires are related to each other as [21]

$$p_x \approx \frac{4l}{j3\omega}I_{0x}, \qquad p_y \approx \frac{4l}{j3\omega}I_{0y}, \tag{17}$$

and solving Eq. (15), the electric and magnetoelectric polarizabilities can be written as

$$\begin{aligned} \alpha_{\text{ee}}^{\text{co}} &= \frac{4l\alpha_1(1-\alpha_5\alpha_6)}{j3\omega(1-\alpha_2\alpha_3-\alpha_5\alpha_6+\alpha_2\alpha_3\alpha_5\alpha_6-\alpha_2\alpha_4\alpha_5\alpha_7)}, \\ \alpha_{\text{ee}}^{\text{cr}} &= \frac{4l\alpha_1\alpha_5\alpha_7}{j3\omega(1-\alpha_2\alpha_3-\alpha_5\alpha_6+\alpha_2\alpha_3\alpha_5\alpha_6-\alpha_2\alpha_4\alpha_5\alpha_7)}, \\ \alpha_{\text{me}}^{\text{co}} &= \frac{\alpha_1\alpha_7}{1-\alpha_2\alpha_3-\alpha_5\alpha_6+\alpha_2\alpha_3\alpha_5\alpha_6-\alpha_2\alpha_4\alpha_5\alpha_7}, \\ \alpha_{\text{me}}^{\text{cr}} &= \frac{\alpha_1\alpha_3(1-\alpha_5\alpha_6)+\alpha_1\alpha_4\alpha_5\alpha_7}{1-\alpha_2\alpha_3-\alpha_5\alpha_6+\alpha_2\alpha_3\alpha_5\alpha_6-\alpha_2\alpha_4\alpha_5\alpha_7}. \end{aligned} \tag{18}$$

It is important to know that the incident electric field can be considered as a uniform external field for the ferrite

sphere as a homogeneous dielectric sphere which has the relative permittivity ε_r. Therefore, an electric dipole moment is induced parallel to the incident field. The absolute value of the moment is given (in the quasistatic approximation) by (e.g., Ref. [31])

$$p = 4\pi a^3 \varepsilon_0 \frac{\varepsilon_r - 1}{\varepsilon_r + 2} E, \tag{19}$$

where ε_0 is the permittivity of free space. Hence, there is an extra electric polarizability which should be added to the cocomponent of the electric polarizability in Eq. (18).

2. Magnetic and electromagnetic polarizabilities

To derive the magnetic and electromagnetic polarizabilities, we assume that there is a high-frequency incident magnetic field in the plane of the particle, for example, in the $\mathbf{x}_0$ direction. This field with the peak value H can excite the magnetic moment of the ferrite sphere. The excited magnetic moment induces an electric current on the metal wires. Similar to the previous process considered above, a coupling cycle is formed because the induced electric currents excite the magnetic moment of the ferrite sphere. The following equations properly explain the cycle as

$$\begin{aligned} I_{0x} &= \alpha_2 m_y, \qquad & m_y &= \alpha_3 I_{0x} + \alpha_4 I_{0y} + \alpha_9 H, \\ I_{0y} &= \alpha_5 m_x, \qquad & m_x &= \alpha_6 I_{0y} + \alpha_7 I_{0x} + \alpha_8 H, \end{aligned} \tag{20}$$

where

$$\alpha_8 = 2\pi a C_{xx}, \qquad \alpha_9 = 2\pi a C_{yx}. \tag{21}$$

Solving Eq. (20) and using Eq. (17) give the magnetic and electromagnetic polarizabilities as

$$\begin{aligned} \alpha_{\mathrm{mm}}^{\mathrm{co}} &= \frac{\alpha_8 - \alpha_2\alpha_3\alpha_8 + \alpha_2\alpha_7\alpha_9}{1 - \alpha_2\alpha_3 - \alpha_5\alpha_6 + \alpha_2\alpha_3\alpha_5\alpha_6 - \alpha_2\alpha_4\alpha_5\alpha_7}, \\ \alpha_{\mathrm{mm}}^{\mathrm{cr}} &= \frac{\alpha_9}{1 - \alpha_2\alpha_3 - \alpha_5\alpha_6 + \alpha_2\alpha_3\alpha_5\alpha_6 - \alpha_2\alpha_4\alpha_5\alpha_7}, \\ \alpha_{\mathrm{em}}^{\mathrm{co}} &= \frac{4l\alpha_2\alpha_9}{j3\omega(1 - \alpha_2\alpha_3 - \alpha_5\alpha_6 + \alpha_2\alpha_3\alpha_5\alpha_6 - \alpha_2\alpha_4\alpha_5\alpha_7)}, \\ \alpha_{\mathrm{em}}^{\mathrm{cr}} &= \frac{4l(\alpha_5\alpha_8(1 - \alpha_2\alpha_3) + \alpha_2\alpha_5\alpha_7\alpha_9)}{j3\omega(1 - \alpha_2\alpha_3 - \alpha_5\alpha_6 + \alpha_2\alpha_3\alpha_5\alpha_6 - \alpha_2\alpha_4\alpha_5\alpha_7)}. \end{aligned} \tag{22}$$

The corresponding coupling block diagram is shown in Fig. 4.

Now, by applying the Onsager-Casimir principle [30]

$$\bar{\bar{\alpha}}_{\mathrm{me}}(\mathbf{H}_0) = -\bar{\bar{\alpha}}_{\mathrm{em}}^{T}(-\mathbf{H}_0), \tag{23}$$

it is possible to obtain the unknown coefficient ξ. $\mathbf{H}_0$ is the internal bias magnetic field, and the superscript T indicates the transpose operation. Using Eq. (23) and considering Eqs. (18) and (22), after simple algebra, the coefficient ξ can be calculated as

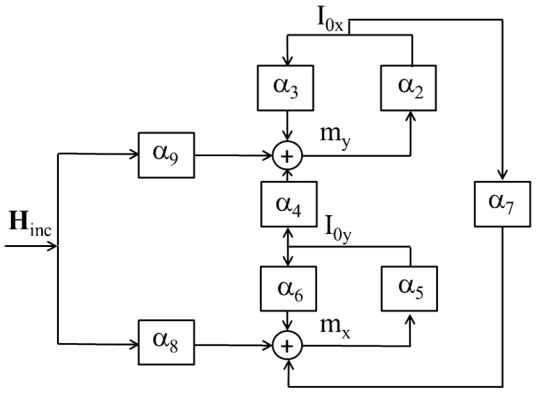

FIG. 4. Block diagram of the coupling between the ferrite inclusion and the metal wires in the Tellegen omega particle in the presence of an incident magnetic field in the $\mathbf{x}_0$ direction.

$$\xi = \frac{-j3\omega\mu_0}{8\pi a}. \tag{24}$$

B. Moving chiral particle

The other particle which has been introduced as the nonreciprocal bianisotropic particle is called the moving chiral. The geometry of the particle is illustrated in Fig. 1(b). Similar to the Tellegen omega particle, the moving chiral particle also consists of two metal wires which are placed on a ferrite inclusion which provides the necessary nonreciprocal response.

1. Electric and magnetoelectric polarizabilities

An incident electric field in the $\mathbf{x}_0$ direction can excite both metal wires because the shorter part of the wire A and the longer part of the wire B are parallel to the $\mathbf{x}_0$ axis. Assuming $l' \ll \lambda$, the small parts of wire A and wire B have approximately uniform current distributions (I_x and I_y, respectively). The long parts of the wires are supposed to be still much smaller than the wavelength. Hence, the wires have approximately the following current distributions:

$$\begin{aligned} I_A &= \begin{cases} I_x\left(1 - \dfrac{y^2}{l^2}\right) & \text{for } |y| > 0 \\ I_x & \text{for } |x| < l', \end{cases} \\ I_B &= \begin{cases} I_y\left(1 - \dfrac{x^2}{l^2}\right) & \text{for } |x| > 0 \\ I_y & \text{for } |y| < l', \end{cases} \end{aligned} \tag{25}$$

in which

$$I_y \approx \frac{l}{Z_{\mathrm{in}}} E, \qquad I_x = \frac{2l'}{Z_{\mathrm{in}}} E. \tag{26}$$

The constant currents I_x and I_y become secondary sources which produce a magnetic field for exciting the ferrite

sphere. The $\mathbf{y}_0$ component of the magnetic field generated by I_x and the $\mathbf{x}_0$ component of the magnetic field generated by I_y have the most principal role in ferrite sphere excitation. Similar to the theory of the Tellegen omega particle, because of the existing nonuniform external magnetic field within the ferrite sphere, the average of the field over the volume of the sphere should be calculated. Using the Biot-Savart law for the short part of wire A (where the current distribution is approximately uniform) and taking the average of the field over the volume of the ferrite sphere gives

$$\begin{aligned} H_{y\ \text{average}} &= \frac{1}{V}\int_V H_y dv \\ &= \frac{I_x}{4\pi V}\int_\pi^{2\pi}\int_0^{\pi}\int_0^{-2a\sin\theta\sin\phi} f(r,\theta,\phi)\,dr d\theta d\phi \\ &= \frac{F}{V}I_x, \\ f(r,\theta,\phi) &= \left(\frac{l'+r\cos\theta}{\sqrt{r^2+l'^2+2rl'\cos\theta}}\right. \\ &\quad \left. + \frac{l'-r\cos\theta}{\sqrt{r^2+l'^2-2rl'\cos\theta}}\right)(-r\sin\phi). \end{aligned} \tag{27}$$

The calculation of the above integral is not straightforward. The value F can be found numerically by, for instance, applying MATLAB simulator software. Similarly, the averaged $\mathbf{x}_0$ component of the external magnetic field due to the constant current I_y can be expressed as

$$H_{x\ \text{average}} = -\frac{F}{V}I_y, \tag{28}$$

in which the sign "−" implies that the produced magnetic field is opposite the $\mathbf{x}_0$ direction. By applying Eqs. (27) and (28) and defining the following coefficients

$$\begin{aligned} C_{xx} = C_{yy} &\triangleq F\left(\frac{\alpha}{\alpha^2+\beta^2}\chi_{xx} + \frac{\beta}{\alpha^2+\beta^2}\chi_{xy}\right), \\ C_{xy} = -C_{yx} &\triangleq F\left(\frac{\alpha}{\alpha^2+\beta^2}\chi_{xy} - \frac{\beta}{\alpha^2+\beta^2}\chi_{xx}\right), \end{aligned} \tag{29}$$

Eq. (9) reduces to

$$m_x = C_{xy}I_x - C_{xx}I_y, \qquad m_y = C_{yy}I_x - C_{yx}I_y, \tag{30}$$

which actually gives the magnetic moment in terms of the constant currents on the short parts of the wires A and B. It is important to appreciate that the excited magnetic moment induces an electric current in the metal wires, because the $\mathbf{y}_0$ component of the magnetic moment produces an external $\mathbf{x}_0$-directed electric field which is tangential to the short part of wire A, and, therefore, it can excite it. The same is true for wire B due to the $\mathbf{x}_0$ component of the magnetic moment. The electric currents in the small parts of the the wires, due to the magnetic moment, can be written as

$$I_x = \frac{\xi}{Z_{\text{in}}}m_y, \qquad I_y = -\frac{\xi}{Z_{\text{in}}}m_x, \tag{31}$$

where ξ is an unknown coefficient. Similar to what we did above for the Tellegen omega particle, this coefficient is found from the Onsager-Casimir principle.

Because the constant currents on the short parts of wires A and B excite the ferrite inclusion, and, simultaneously, the magnetic moment induces an electric current on the wires, a coupling cycle is created, which is illustrated by the block diagram in Fig. 5. The coupling cycle can be also expressed mathematically as the following relations:

$$\begin{aligned} I_x &= \alpha_8' E + \alpha_2 m_y, \qquad m_y = \alpha_3 I_x + \alpha_4 I_y, \\ I_y &= \alpha_5 m_x + \alpha_1 E, \qquad m_x = \alpha_6 I_y + \alpha_7 I_x, \end{aligned} \tag{32}$$

where

$$\begin{aligned} \alpha_1 &\approx \frac{l}{Z_{\text{in}}}, \qquad \alpha_2 = -\alpha_5 = \frac{\xi}{Z_{\text{in}}}, \\ \alpha_3 &= C_{yy}, \qquad \alpha_4 = -C_{yx}, \\ \alpha_6 &= -C_{xx}, \qquad \alpha_7 = C_{xy}, \qquad \alpha_8' = \frac{2l'}{Z_{\text{in}}}. \end{aligned} \tag{33}$$

The electric dipole moments and the constant electric currents in the short parts of the wires are related to each other as

$$p_x \approx \frac{4l}{j3\omega}I_y + \frac{2l'}{j\omega}I_x, \qquad p_y \approx \frac{2l'}{j\omega}I_y - \frac{4l}{j3\omega}I_x. \tag{34}$$

Using Eq. (32) and also considering Eq. (34), the electric and magnetoelectric polarizabilities can be written as

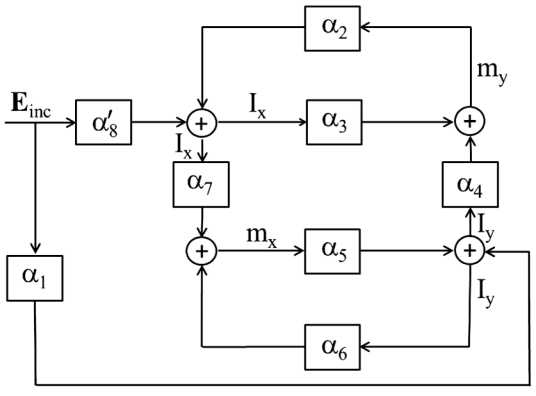

FIG. 5. Block diagram of the coupling between the metal wires and the ferrite inclusion in the moving chiral particle in the presence of an incident electric field in the $\mathbf{x}_0$ direction.

$$\alpha_{ee}^{co} = \frac{4l}{j3\omega}A_y + \frac{2l'}{j\omega}A_x, \qquad \alpha_{ee}^{cr} = \frac{2l'}{j\omega}A_y - \frac{4l}{j3\omega}A_x,$$
$$\alpha_{me}^{co} = \frac{\alpha_1\alpha_6(1-\alpha_2\alpha_3) + \alpha_1\alpha_2\alpha_4\alpha_7 + \alpha_7\alpha_8'}{1-\alpha_2\alpha_3-\alpha_5\alpha_6+\alpha_2\alpha_3\alpha_5\alpha_6-\alpha_2\alpha_4\alpha_5\alpha_7},$$
$$\alpha_{me}^{cr} = \frac{\alpha_3\alpha_8'(1-\alpha_5\alpha_6) + \alpha_1\alpha_4 + \alpha_4\alpha_5\alpha_7\alpha_8'}{1-\alpha_2\alpha_3-\alpha_5\alpha_6+\alpha_2\alpha_3\alpha_5\alpha_6-\alpha_2\alpha_4\alpha_5\alpha_7}, \tag{35}$$

in which the coefficients A_x and A_y read

$$A_x = \frac{\alpha_8'(1-\alpha_5\alpha_6) + \alpha_1\alpha_2\alpha_4}{1-\alpha_2\alpha_3-\alpha_5\alpha_6+\alpha_2\alpha_3\alpha_5\alpha_6-\alpha_2\alpha_4\alpha_5\alpha_7},$$
$$A_y = \frac{\alpha_1(1-\alpha_2\alpha_3) + \alpha_5\alpha_7\alpha_8'}{1-\alpha_2\alpha_3-\alpha_5\alpha_6+\alpha_2\alpha_3\alpha_5\alpha_6-\alpha_2\alpha_4\alpha_5\alpha_7}. \tag{36}$$

2. Magnetic and electromagnetic polarizabilities

Most of the formulas given above can be used, and we need only to rewrite the relations between the constant currents and the magnetic moment as

$$I_x = \alpha_2 m_y, \qquad m_y = \alpha_3 I_x + \alpha_4 I_y + \alpha_9 H,$$
$$I_y = \alpha_5 m_x, \qquad m_x = \alpha_6 I_y + \alpha_7 I_x + \alpha_8 H. \tag{37}$$

Here, H is the peak value of the high-frequency incident magnetic field. If we assume that this incident magnetic field has only an $\mathbf{x}_0$ component, then

$$\alpha_8 = \frac{4\pi a^3}{3F}C_{xx}, \qquad \alpha_9 = \frac{4\pi a^3}{3F}C_{yx}. \tag{38}$$

By applying Eqs. (34) and (37), the magnetic and electromagnetic polarizabilities can be expressed as

$$\alpha_{mm}^{co} = \frac{\alpha_8(1-\alpha_2\alpha_3)+\alpha_2\alpha_7\alpha_9}{1-\alpha_2\alpha_3-\alpha_5\alpha_6+\alpha_2\alpha_3\alpha_5\alpha_6-\alpha_2\alpha_4\alpha_5\alpha_7},$$
$$\alpha_{mm}^{cr} = \frac{\alpha_9}{1-\alpha_2\alpha_3-\alpha_5\alpha_6+\alpha_2\alpha_3\alpha_5\alpha_6-\alpha_2\alpha_4\alpha_5\alpha_7},$$
$$\alpha_{em}^{co} = \frac{4l}{j3\omega}B_y + \frac{2l'}{j\omega}B_x, \quad \alpha_{em}^{cr} = \frac{2l'}{j\omega}B_y - \frac{4l}{j3\omega}B_x, \tag{39}$$

where the coefficients B_x and B_y are given by

$$B_x = \frac{\alpha_2\alpha_9}{1-\alpha_2\alpha_3-\alpha_5\alpha_6+\alpha_2\alpha_3\alpha_5\alpha_6-\alpha_2\alpha_4\alpha_5\alpha_7},$$
$$B_y = \frac{\alpha_5\alpha_8(1-\alpha_2\alpha_3)+\alpha_2\alpha_5\alpha_7\alpha_9}{1-\alpha_2\alpha_3-\alpha_5\alpha_6+\alpha_2\alpha_3\alpha_5\alpha_6-\alpha_2\alpha_4\alpha_5\alpha_7}. \tag{40}$$

As it is seen from Eq. (37), the coupling block diagram for this case is completely similar to what is shown in Fig. 4 for the Tellegen omega particle. The coefficients α_2 and α_5, which show the effect of the magnetic moment on the metal wires, are determined by the Onsager-Casimir principle. After some algebraic manipulations, we get

$$\alpha_2 = -\alpha_5 = \mu_0 \frac{\alpha_1\alpha_4 + \alpha_3\alpha_8'}{\left(\frac{4l}{j3\omega}\right)\alpha_9 - \left(\frac{2l'}{j\omega}\right)\alpha_8}. \tag{41}$$

III. RESULTS AND DISCUSSION

Here, we consider the polarizablities of three example particles described in Table I, compare the analytical predictions with numerical simulations, and discuss the results.

A. Tellegen omega particle

As an example, we study the properties of the particles whose constituent material properties and dimensions are illustrated in Table I, part (a). For having the resonance

TABLE I. Nonreciprocal bianisotropic particles, properties, and dimensions.

(a) Tellegen omega particle
Resonance frequency at 10 GHz

Ferrite material	Saturation magnetization	ε_r	$\mathbf{H}_a$	a	$2l$
YIG	1780 G	15	3570 Oe	0.5 mm	3.0 mm

(b) Moving chiral particle
Resonance frequency at 2.5 GHz

Ferrite material	Saturation magnetization	ε_r	$\mathbf{H}_a$	a	$2l'$	l
YIG	1780 G	15	892.5 Oe	0.5 mm	1.2 mm	6.9 mm

(c) Moving chiral particle
Resonance frequency at 2 GHz

Ferrite material	Saturation magnetization	ε_r	$\mathbf{H}_a$	a	$2l'$	l
YIG	1780 G	15	714 Oe	0.5 mm	3 mm	9 mm

frequency at 10 GHz, the bias magnetic field should be 3570 Oe. The ferrite material is assumed to be moderately lossy with the damping factor equal to 0.001. The length of each wire is 3 mm, which is one-tenth of the wavelength. Hence, the current distribution considered in Eq. (4) is a valid model. To confirm the analytical results, we find the polarizabilities also numerically based on the approach developed in Ref. [32]. Simulations are done by the finite element method applying ANSYS HFSS software. Simulations can be done using the method of moment also. Figure 6 compares the analytical polarizabilities with the numerical ones. As it is seen, the resonance frequency is approximately 10 GHz, and the simulated and analytical results are fairly well matched.

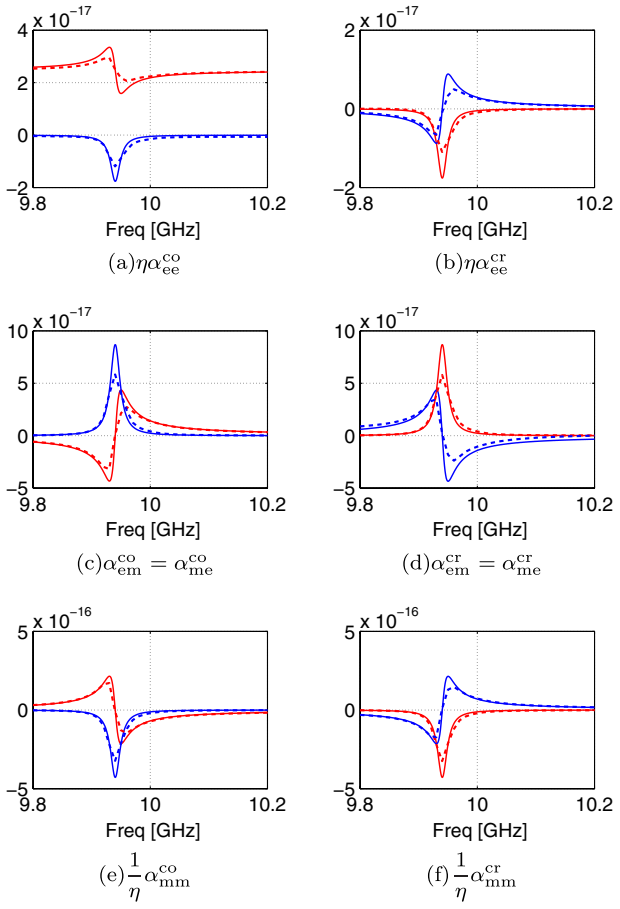

FIG. 6. Comparison of the simulated and analytical polarizabilities of the Tellegen omega particle. Solid lines are the analytical polarizabilities and dashed lines are the simulated polarizabilities. Red and blue colors represent the real and imaginary parts of the polarizability, respectively. (a) Normalized cocomponent of the electric polarizability; (b) normalized cross component of the electric polarizability; (c) normalized cocomponents of the electromagnetic and magnetoelectric polarizabilities; (d) normalized cross components of the electromagnetic and magnetoelectric polarizabilities; (e) normalized cocomponent of the magnetic polarizability; (f) normalized cross component of the magnetic polarizability.

B. Moving chiral particle

In this example, we assume that the long parts of the wires (l) are large compared to l' but small compared to the wavelength. Hence, we need to decrease the resonance frequency used in the example of the Tellegen omega particle (10 GHz) to be able to increase the value of l, so that the wavelength will be still larger than the size of the particle. Therefore, 2.5 GHz can be a reasonable choice corresponding the wavelength 120 mm. The ferrite material is the same as above (the same relative permittivity, the saturation magnetization, and damping factor). For having the resonance at 2.5 GHz, the applied bias field is 892.5 Oe. We assume $l' = 0.6$ mm and $l = 6.9$ mm [Table I, part (b)]. The analytical results for the particle are compared with the simulated ones in Figs. 7 and 8. Figure 7 shows the electric and the magnetic polarizabilities, and Fig. 8 shows the electromagnetic and the magnetoelectric polarizabilities. As it is clear in the figures, there is a very small difference in the resonance frequency between the analytical and the simulated results. That can be because of an inaccuracy in calculating the applied bias field for having the resonance at 2.5 GHz. However, it is thought that the main source of that shift is in the inaccuracies of determining the reactive part of the input impedances of the wire elements. The analytical polarizabilities α_{ee}^{co}, α_{ee}^{cr}, α_{mm}^{co}, and α_{mm}^{cr} are nicely

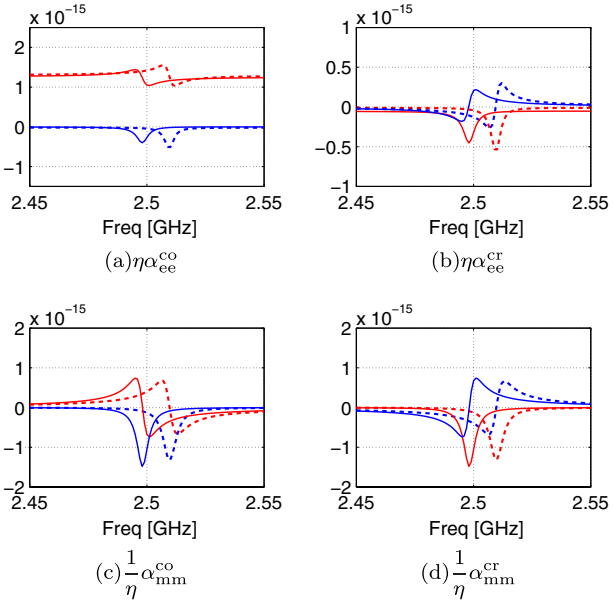

FIG. 7. Comparison of the analytical and simulated (electric and magnetic) polarizabilities of the moving chiral particle with $l = 6.9$ mm and $l' = 0.6$ mm. Solid lines are the analytical polarizabilities and dashed lines are the simulated polarizabilities. Red and blue colors represent the real and imaginary parts of the polarizability, respectively. (a) Normalized cocomponent of the electric polarizability; (b) normalized cross component of the electric polarizability; (c) normalized cocomponent of the magnetic polarizability; (d) normalized cross component of the magnetic polarizability.

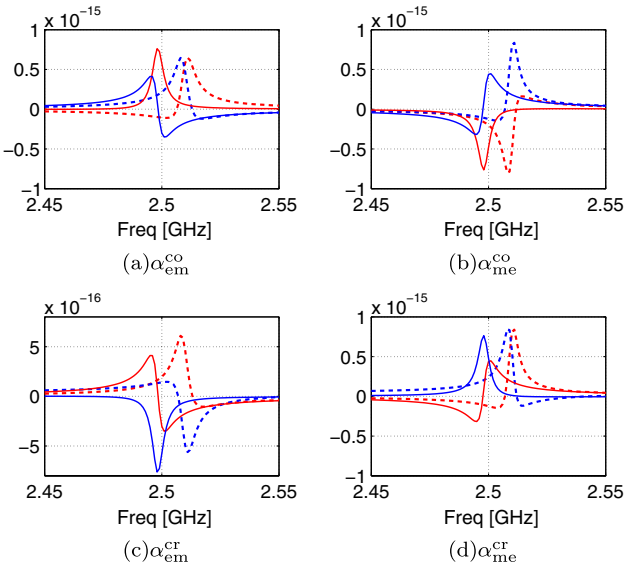

FIG. 8. Comparison of the analytical and simulated (electromagnetic and magnetoelectric) polarizabilities of the moving chiral particle with $l = 6.9$ mm and $l' = 0.6$ mm. Solid lines are the analytical polarizabilities and dashed lines are the simulated polarizabilities. Red and blue colors represent the real and imaginary parts of the polarizability, respectively. (a) Normalized cocomponent of the electromagnetic polarizability; (b) normalized cocomponent of the magnetoelectric polarizability; (c) normalized cross component of the electromagnetic polarizability; (d) normalized cross component of the magnetoelectric polarizability.

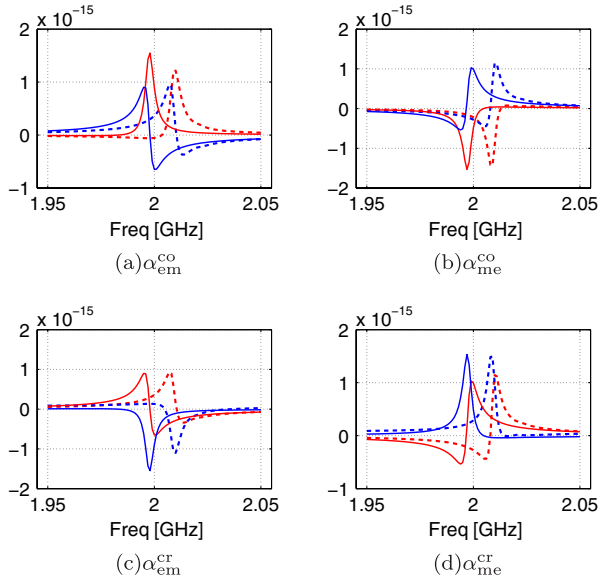

FIG. 9. Comparison of the analytical and simulated (electromagnetic and magnetoelectric) polarizabilities of the moving chiral particle with $l = 9$ mm and $l' = 1.5$ mm. Solid lines are the analytical polarizabilities and dashed lines are the simulated polarizabilities. Red and blue colors represent the real and imaginary parts of the polarizability, respectively. (a) Normalized cocomponent of the electromagnetic polarizability; (b) normalized cocomponent of the magnetoelectric polarizability; (c) normalized cross component of the electromagnetic polarizability; (d) normalized cross component of the magnetoelectric polarizability.

matched in value and behavior with the simulated results. Next, let us discuss the behavior of the electromagnetic and magnetoelectric polarizabilities, where we observe differences between the analytical and simulated results.

If we focus only on the analytical results, we find that the polarizabilities $\alpha_{\rm em}^{\rm co}$ and $\alpha_{\rm me}^{\rm co}$ or the polarizabilities $\alpha_{\rm em}^{\rm cr}$ and $\alpha_{\rm me}^{\rm cr}$ are not exactly opposite each other in the whole frequency range from 2.45 to 2.55 GHz. For a pure moving chiral particle, we should have $\alpha_{\rm em}^{\rm co} = -\alpha_{\rm me}^{\rm co}$ (chiral property) and $\alpha_{\rm em}^{\rm cr} = -\alpha_{\rm me}^{\rm cr}$ (moving property). In fact, with the structure of our particle, there are also couplings of the other two types, Tellegen and omega, in addition to the moving and chiral ones. The fundamental reason for the existing Tellegen and omega coupling effects is the central (short) parts of the wires close to the ferrite inclusion. Therefore, we observe mixing of all four coupling phenomena and not a pure moving chiral particle. Looking at the simulated results for the electromagnetic and magnetoelectric polarizabilities, we see that this is more pronounced in the numerical results. We think that in addition to this topology effect, the long arms of the wires are very close to the ferrite inclusion and they can create parasitic effects in the ferrite sphere excitation (due to strong nonuniformity of the fields). In theory, we have not taken into account these parasitic effects, and, therefore, the differences of the numerical electromagnetic and magnetoelectric polarizabilities and the theoretical ones are not negligible. Hence, we should find a way to reduce the impact of the long arms of the wires, and one possible solution is moving them farther away from the ferrite sphere by increasing the length of the central part of the wires. We study an example case with $l' = 1.5$ mm [Table I, part (c)]. As mentioned before, l is assumed to be much larger than l'. To realize this, we suppose that l is 6 times larger than l', which gives $l = 9$ mm. Because the size of the particle should be much smaller than the wavelength, we replace 2.5 GHz with 2 GHz as the resonance frequency. The corresponding applied bias field is 714 Oe. Figure 9 presents the real and imaginary parts of the electromagnetic and the magnetoelectric polarizabilities obtained analytically and numerically for this example.

As it is seen, now there is fairly good agreement between the analytical and simulated results. Still, because of inevitable inaccuracies, a little difference exists in the resonance frequencies. The parasitic effects have been mainly removed, but, naturally, the Tellegen and omega coupling effects remain significant.

IV. CONCLUSION

In this work, we apply the antenna theory concepts (for electrically small short-circuit wire antennas) and the

knowledge about electromagnetic properties of ferrite materials to derive analytically the electric, magnetic, electromagnetic, and magnetoelectric polarizabilities of two artificial nonreciprocal bianisotropic particles named Tellegen omega and moving chiral. The results provide analytical means to predict electromagnetic response for particles of given topology and sizes, opening a way to design particles with the desired bianisotropic parameters, as required for applications. More specifically, in these particles, the values of all the polarizabilities can be engineered by properly choosing the topology and sizes of the metal parts and the parameters of the magnetized ferrite sphere. We study the excitations of these particles in incident uniform electric fields in the plane of the particles and find the electric and magnetoelectric polarizabilities. Studies of excitations by incident uniform magnetic fields allow us to derive the magnetic and electromagnetic polarizabilities. Subsequently, we compare the analytical results with the simulated ones. For the Tellegen omega particle, which has a simpler topology, the analytical polarizabilities show very good agreement with the numerical polarizabilities. For the moving chiral particle, because of the complex shape of the metal parts, parasitic effects due to field inhomogeneities are more significant, and initially the analytical results do not agree well with the simulated results. However, we show that optimization of the particle dimensions allows us to reduce the parasitic interactions, and we observe that the analytical and simulated results are almost identical for the optimized particle. A comparison of the electromagnetic and magnetoelectric polarizabilities for the particle indicates that the particle exhibits also some Tellegen and omega coupling effects.

In the future, we hope to confirm the analytical and numerical polarizabilities experimentally. By developing waveguide measurement techniques and placing such particles inside a waveguide with different orientations, it is thought that it can be possible to find all the relevant components of the particle polarizabilities. The other important research problem is to find a possible means to control different magnetoelectric coefficients independently, so that any desired (physically possible) values of the parameters will be at reach. As we see from the results of this paper, the example "moving" particle shows also some degree of Tellegen and omega coupling, which may be detrimental for some potential applications. We hope that this paper is a significant step towards the future use of nonreciprocal bianisotropic particles in microwave devices, such as nonreciprocal perfect absorbers or nonreciprocal thin-sheet isolators [8,10–12].

[1] A. N. Serdyukov, I. V. Semchenko, S. A. Tretyakov, and A. Sihvola, *Electromagnetics of Bianisotropic Materials: Theory and Applications* (Gordon and Breach Science Publishers, Amsterdam, 2001).

[2] C. M. Soukoulis and M. Wegener, Past achievements and future challenges in the development of three-dimensional photonic metamaterials, Nat. Photonics **5**, 523 (2011).

[3] Z. Li, M. Mutlu, and E. Ozbay, Chiral metamaterials: From optical activity and negative refractive index to asymmetric transmission, J. Opt. **15**, 023001 (2013).

[4] Y. Ra'di and S. A. Tretyakov, Balanced and optimal bianisotropic particles: Maximizing power extracted from electromagnetic fields, New J. Phys. **15**, 053008 (2013).

[5] J. Vehmas, Y. Ra'di, A. Karilainen, and S. A. Tretyakov, Eliminating electromagnetic scattering from small particles, IEEE Trans. Antennas Propag. **61**, 3747 (2013).

[6] S. A. Tretyakov, Physical interpretation of the transparent absorbing boundary for the truncation of the computational domain, IEEE Microwave Guided Wave Lett. **8**, 321 (1998).

[7] J. Peng and C. A. Balanis, Transparent absorbing boundary (TAB) for the truncation of the computational domain, IEEE Microwave Guided Wave Lett. **7**, 347 (1997).

[8] Y. Ra'di, V. S. Asadchy, and S. A. Tretyakov, Total absorption of electromagnetic waves in ultimately thin layers, IEEE Trans. Antennas Propag. **61**, 4606 (2013).

[9] T. Niemi, A. O. Karilainen, and S. A. Tretyakov, Synthesis of polarization transformers, IEEE Trans. Antennas Propag. **61**, 3102 (2013).

[10] Y. Ra'di, V. S. Asadchy, and S. A. Tretyakov, One-way transparent sheets, Phys. Rev. B **89**, 075109 (2014).

[11] Y. Ra'di, V. S. Asadchy, and S. A. Tretyakov, arXiv: 1401.1677.

[12] S. A. Tretyakov, I. S. Nefedov, and P. Alitalo, Generalized field-transforming metamaterials, New J. Phys. **10**, 115028 (2008).

[13] D. N. Astrov, Magnetoelectric effect in chromium oxide, Sov. Phys. JETP **13**, 729 (1961).

[14] B. D. H. Tellegen, The gyrator, a new electric network element, Philips Res. Rep. **3**, 81 (1948).

[15] I. V. Lindell, A. H. Sihvola, S. A. Tretyakov, and A. J. Viitanen, *Electromagnetic Waves in Chiral and Bi-isotropic Media* (Artech House, Norwood, MA, 1994).

[16] E. O. Kamenetskii, On the technology of making chiral and bianisotropic waveguides for microwave propagation, Microw. Opt. Technol. Lett. **11**, 103 (1996).

[17] V. Dmitriev, Constitutive tensor nomenclature of Kamenetskii's media, Microwave Opt. Technol. Lett. **18**, 280 (1998).

[18] S. A. Tretyakov, Nonreciprocal composite with the material relations of the transparent absorbing boundary, Microw. Opt. Technol. Lett. **19**, 365 (1998).

[19] S. A. Tretyakov, S. I. Maslovski, I. S. Nefedov, A. J. Viitanen, P. A. Belov, and A. Sanmartin, Artificial Tellegen particle, Electromagnetics **23**, 665 (2003).

[20] S. A. Tretyakov, A. H. Sihvola, A. A. Sochava, and C. R. Simovski, Magnetoelectric interactions in bianisotropic media, J. Electromagn. Waves Appl. **12**, 481 (1998).

[21] S. A. Tretyakov, S. Maslovski, and P. A. Belov, An analytical model of metamaterials based on loaded wire dipoles, IEEE Trans. Antennas Propag. **51**, 2652 (2003).

[22] R. W. P. King and C. W. Harrison, *Antennas and Waves: A Modern Approach* (MIT Press, Cambridge, MA, 1969).

[23] J. D. Jackson, *Classical Electrodynamics* (John Wiley & Sons, New York, 1999).

[24] W. K. H. Panofsky and M. Phillips, *Classical Electricity and Magnetism* (Addison-Wesley, Reading, MA, 1955).
[25] D. K. Cheng, *Field and Wave Electromagnetics* (Addison-Wesley, Reading, MA, 1989).
[26] D. M. Pozar, *Microwave Engineering* (John Wiley & Sons, New York, 2005).
[27] R. E. Collin, *Foundations for Microwave Engineering* (John Wiley & Sons, New York, 2001).
[28] L. Onsager, Reciprocal relations in irreversible processes, Phys. Rev. **37**, 405 (1931).
[29] H. B. G. Casimir, On Onsager's principle of microscopic reversibility, Rev. Mod. Phys. **17**, 343 (1945).
[30] S. V. Zagriadski and S. A. Tretyakov, *Proceedings of the 31st European Microwave Conference, London, UK, 2001* (Microwave Engineering Europe, CMP Europe Ltd., London, 2001), pp. 1–4.
[31] A. Sihvola, *Electromagnetic Mixing Formulas and Applications* (The Institution of Electrical Engineers, London, 1999).
[32] V. S. Asadchy, I. A. Faniayeu, Y. Ra'di, and S. A. Tretyakov, arXiv:1401.4930.